New York Science Journal

Websites:
http://www.sciencepub.net/newyork
http://www.sciencepub.net

Emails:
newyorksci@gmail.com
editor@sciencepub.net

MARSLAND PRESS
Multidisciplinary Academic Journal Publisher

Preparation and Modification of $MnCo_2O_4$ Spinel Electro catalyst for OER

Rajbhandari Bijina

School of Materials Science and Engineering, Nanjing University of Science and Technology, Nanjing, Jiangsu 210094, PR China
bzna55@yahoo.com

Abstract: Taxonomic Electrochemical energy storage devices such as zinc air batteries and alkaline fuel cells are on a growth trajectory which cost less to operate. For the improvement of a number of renewable energy technologies, including metal-air batteries improved catalyst for the OER are required. One of key factors in OER improvement is the increasing the specific surface area. Here, the synthesis of $MnCo_2O_4$/MWCNT composite fabricated by the electrospinning methods with enhanced surface area, is presented. Corresponding characterizations by SEM, WRD, BET, XPS of $MnCo_2O_4$/MWCNTs prepared through electrospinning method, reveal the formation of higher specific surface area comparing to $MnCo_2O_4$ and $MnCo_2O_4$/MWCNT composites prepared by hydrothermal method. All samples were utilized as oxygen evolution reaction (OER) catalysts for electro catalytic H_2 generation through water electrolysis. A quite low over potential of 520 mV is required to attain a current density of 10 mA/cm^2, with a Tafel slope of 114 mVdec^{-1} for OER in 1 M KOH solution.
[Rajbhandari Bijina. **Preparation and Modification of $MnCo_2O_4$ Spinel Electro catalyst for OER.** *N Y Sci J* 2020;13(6):9-18]. ISSN 1554-0200 (print); ISSN 2375-723X (online). http://www.sciencepub.net/newyork. 2. doi:10.7537/marsnys130620.02.

Keywords: $MnCo_2O_4$, MWCNT, Hydrothermal, Electrospinning, Metal-air battery, OER

1. Introduction

The adverse environmental effects of fossil-fuel-based energy systems, their sustainability issues and increasing demands have given impetus to research into advanced energy conversion and storage systems [1] [2]. It is necessary to develop energy storage devices such as batteries, capacitors, fuel cells and supercapacitors that play important roles in the application of renewable energy in order to make the energy stable and meet the energy demand [3] [4]. The industrialization of Li-air system faces numerous safety and stability issues due to highly reactive nature of lithium although this battery has the highest theoretical energy density. Because of its high energy density which is about 4 times higher than the Li-ion battery, non-toxicity and abundance of Zn in the earth's crust Zn-air battery is best choice for commercialization [5] [6]. One of the most important reactions is oxygen evolution reaction (OER). Recently, the best electro catalysts for OER are noble metal oxides like IrO_2 or RuO_2 with their high cost, scarcity, and instable catalytic performance restrict those wide application [7]. Therefore, developing an efficient non noble metal oxide OER catalyst is emergent. Various studies have been reported the spinel-type metal cobaltite systems whose chemical formulas are MCo_2O_4 such as Co_3O_4, $MnCo_2O_4$, $NiCo_2O_4$, $ZnCo_2O_4$ and so on. Those received interest due to their high theoretical capacity [8]. Among them, $MnCo_2O_4$ are the superior capacity performance nevertheless their particle applications are still low conductivity, poor stability, and imperfect durability during the charging/discharging process [9]. To improve the electrochemical property, many methods such as conductive material namely graphene sheet [10], reduced graphene oxide (rGO) [11], multi-wall carbon nanotubes (MWCNT's) were used [12]. In Addition, several studies indicated the mixed transition metal oxides with hollow/porous structure lead to enhance near-surface storage capacity and activity. Thus, the electrospinning formation pathway of the synthesized fibrous tubular structures was found to be different from the existing heterogeneous contraction mechanism which affects the final morphology structures [13]. In this study, $MnCo_2O_4$ and $MnCo_2O_4$/MWCNT composited catalysts synthesized by the hydrothermal and electrospinning methods are compared the performance in terms of enhancing the OER. To clarify the inherent mechanisms, involving the high specific surface of $MnCo_2O_4$/MWCNT by electrospinning methods, the role of conducting MWCNT in the composite catalysts. The $MnCo_2O_4$/MWCNT composited catalyst prepared through different methods leads to the different values of the specific surface area which directly affect to enhance the OER. The

characterization and electrochemical properties of those prepared catalysts were observed by SEM, XRD, BET, XPS, LSV and CV.

2. Materials and experiments

2.1 The Experiments

2.1.1 Preparation of $MnCo_2O_4$ and $MnCo_2O_4$/MWCNTs

Hydrothermal method: 0.5 mmol of manganese acetate and 1 mmol of cobalt nitrate were mixed in 60 ml of deionized water, then 0.01 mmol of urea were added. The suspension was continually stirred until the solution turns clear pink. After that transfer the obtained solution to a 100 ml hydrothermal kettle and put into the constant temperature oven temperature for 8 hours under the condition of 120 ℃. Clean it with deionized water and anhydrous ethanol for three times, then put the obtained solution into the oven and dry it at 80 ℃. The precursor was put into muffle furnace, kept at 400 ℃ for 2 hours at 2 ℃/min of heating rate.

Electrospinning method: 5 g of absolute ethanol and 5 g of DMF were mixed and stirred by magnetic stirrer. Then 0.5 mmol of manganese acetate and 1 mmol of cobalt nitrate were added and continued stirring for half an hour until all are dissolved. After that 1 gram of PVP was slowly added and stirred for 3 hours to make the solution uniform. The solution was transferred into a 10 ml syringe, load the needle and connect the high-voltage power supply working at 20 kV of voltage, 15 cm plate spacing and 1 ml/h spinning speed. The spinning precursor was put into the muffle furnace for 2 hours at 400℃ (2℃ per minute of heating speed).

To prepare $MnCo_2O_4$/MWCNTs, 0.5 g of the prepared $MnCo_2O_4$ was dispersed in 20 ml ethanol by ultrasonication for 30 minutes. To the well-dispersed MnCo2O4 suspension, 5 wt % of MWCNT was added and further sonicated for 4hours. Later, the suspension was allowed to dry in an oven maintained at 80 °C.

2.1.2 Basic characterizations

X-ray diffraction analyzer (SHIMADZU, LabX XRD-6100.) was performed at working voltage of 40KV and working current of 30 mA with a scanning angle range of 20-80° (6°/min), using Cu-Kα radiation. Scanning Electron Microscope (SEM, Quant 250FEG) was performed at a test voltage of 20 kV with amplification of 3000-100000 times. X-ray photoelectron spectroscopy (XPS, Thermo, ESCALAB 250Xi) was performed the monochromatic AL Kaa (hvn = 1486.6 eV) with the power of 150 W. The fixed transmission energy of 500 μm with beam spot energy analyzer is 30 eV. Brunauer-Emmett-Teller specific surface analyzer (BET, Gemini VII 2390) used to measure the nitrogen adsorption and desorption on the powder samples at 77 K.

2.1.3 Electrochemical characterizations

The working electrodes were prepared by depositing active catalyst suspensions onto a glassy carbon (GC, 0.07 cm^2) using a micro injector. The suspensions were prepared by mixing 20 mg catalyst, 20 mg conductive carbon, 1 mL DI water, 1 mL isopropanol and 40 μL Nafion solution (5 wt %) and sonicated for 1 h to homogenize. A 4 μL aliquot of this suspension was drop-cast onto the GC disk electrode and left to dry under an inverted beaker in natural conditions. The typical catalyst loading was 0.035 mg cm^{-2}.

All electrochemical measurements were performed in a conventional three-electrode system on an electrochemical station (CHI 660e). The GC electrode within catalysts ink, Platinum (Pt) wire and Ag|AgCl (3.5 M KCl) electrode were used as working electrode, counter electrode and reference electrode, respectively. In ECSA tests, the electrolyte (0.1 M KOH) was introduced N_2 for 30 min to empty O_2, while other tests would introduced O_2 for 30 min another to ensure O_2 is saturated, and maintained introducing O_2 throughout the test. Polarization curves were obtained using linear sweep voltammetry (LSV) measurements performed on a rotating disk electrode (RDE) at 1600 rpm, at a scan rate of 5 mV s^{-1} from 0 to 1 V vs. Ag|AgCl (3.5 M KCl). In order to ensure the electrodes ran steadily, cyclic voltammogram (CV) had been performed from -1 to 1 V vs. Ag|AgCl (3.5 M KCl) for 50 times even more till reproducible curves were observed. The electrochemical impedance spectra (EIS) measurements were performed at 0.7 V vs. Ag|AgCl (3.5 M KCl), in the frequency range of 100 kHz to 0.01 Hz under an AC voltage of 5 mV. The electrochemical specific surface (ECSA) test was performed by CV measurements in a non-faradic current region (0.25-0.35 V vs. Ag|AgCl) at scan rates of 2, 4, 6, 8, 10 mV s^{-1}. The stability of samples were performed by chronopotentiometry measurement at 10 mA cm^{-2} for 7200 seconds, which can evaluate a catalyst's activity and short term stability [14].

3. Result and discussion

Characterization

The morphology of prepared MnCo2O4 and MnCo2O4/MWCNT composite powders were investigated using scanning electron microscopy (SEM), as shown in Figure 1.

As the SEM images in Figure 1 (a) and (b) displayed the morphology of MnCo2O4 and MnCo2O4/MWCNT prepared by the electrospinning method (E-MnCo2O4 and E-MnCo2O4/MWCNT), respectively.

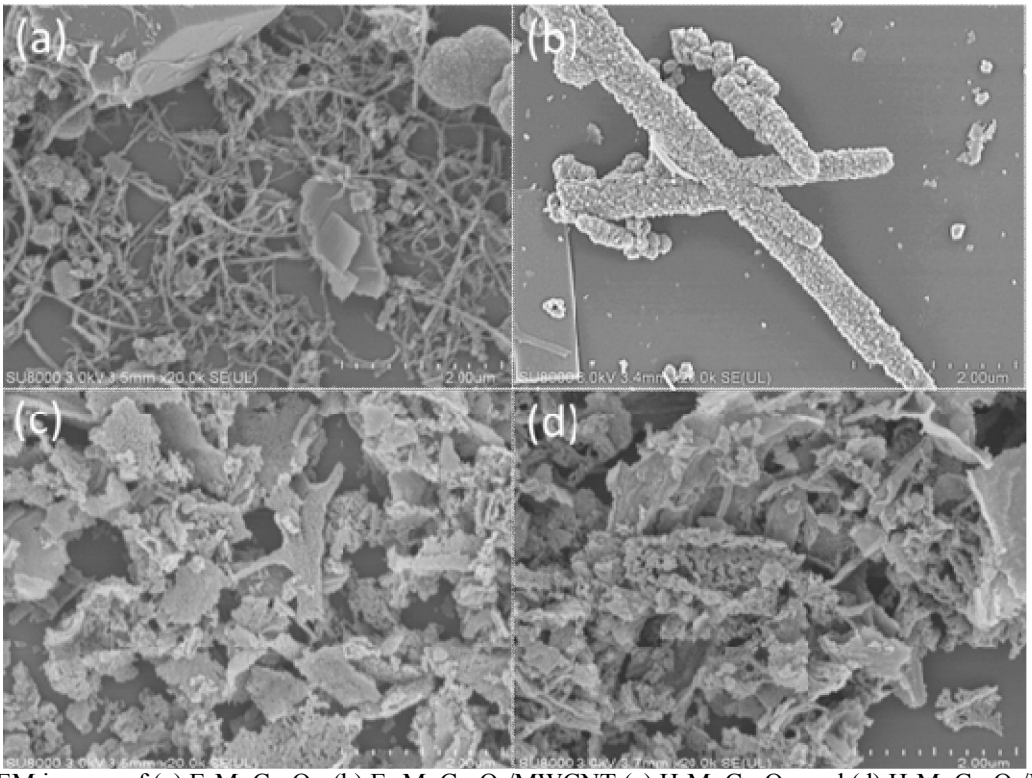

Figure 1 SEM images of (a) E-$MnCo_2O_4$, (b) E- $MnCo_2O_4$/MWCNT (c) H-$MnCo_2O_4$, and (d) H-$MnCo_2O_4$/MWCNT

Both samples showed the typical fibrous morphologies with a thickness of approximately 0.2 µm for E-MnCo2O4 and approximately 1 µm for E-MnCo2O4/MWCNT. Decorating of MWCNT layers made the E-MnCo2O4/MWCNT fibers thicker than those pure. Figure 1 (c) and (d) presented the morphology of MnCo2O4 and MnCo2O4/MWCNT prepared by the hydrothermal method (H-MnCo2O4 and H-MnCo2O4/MWCNT), respectively. Both samples exhibited amorphous particles in the agglomerated state. The morphology of H-MnCo2O4 and H-MnCo2O4/MWCNT display the particle size similarly.

To characterize the crystalline structure of synthesized MnCo2O4 and MnCo2O4/MWCNT composite, X-ray diffraction (XRD) was operated at an operating voltage of 40 kV and working current of 30 mA within a range of 20-80 ° with an interval of 0.02 ° using Cu-Kα radiation.

As Figure 2 showed XRD patterns of all sample. Those indicated the sharp peak at (311), 2θ=35.995 which corresponded to the main peck of Manganese cobalt oxide ($MnCo_2O_4$) and other peaks such as (111), (220), (400), (422), (511) and (440) were concurrence to the pure phase of $MnCo_2O_4$. Following the standard data of $MnCo_2O_4$ (JCPDS No. 23-1237), their XRD patterns indexed as a face-centered cubic structure of $MnCo_2O_4$ with the space group fd3m [15]. The XRD of H-$MnCo_2O_4$/MWCNT and E-$MnCo_2O_4$/MWCNT presents the peak at 26.14 ° (002) which corresponded to the main peak of pristine MWCNT.

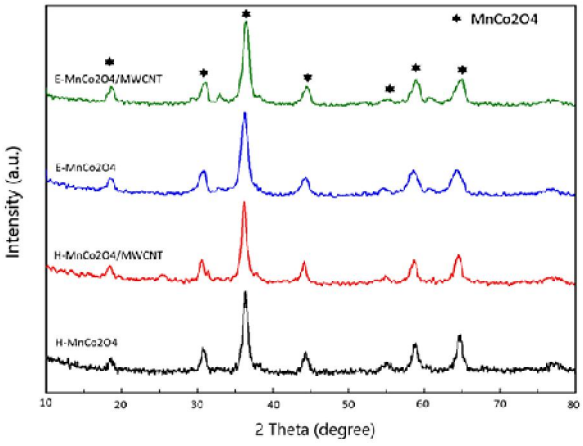

Figure 2 XRD patterns E-$MnCo_2O_4$, E- $MnCo_2O_4$ /MWCNT, H-$MnCo_2O_4$, and H-$MnCo_2O_4$/MWCNT

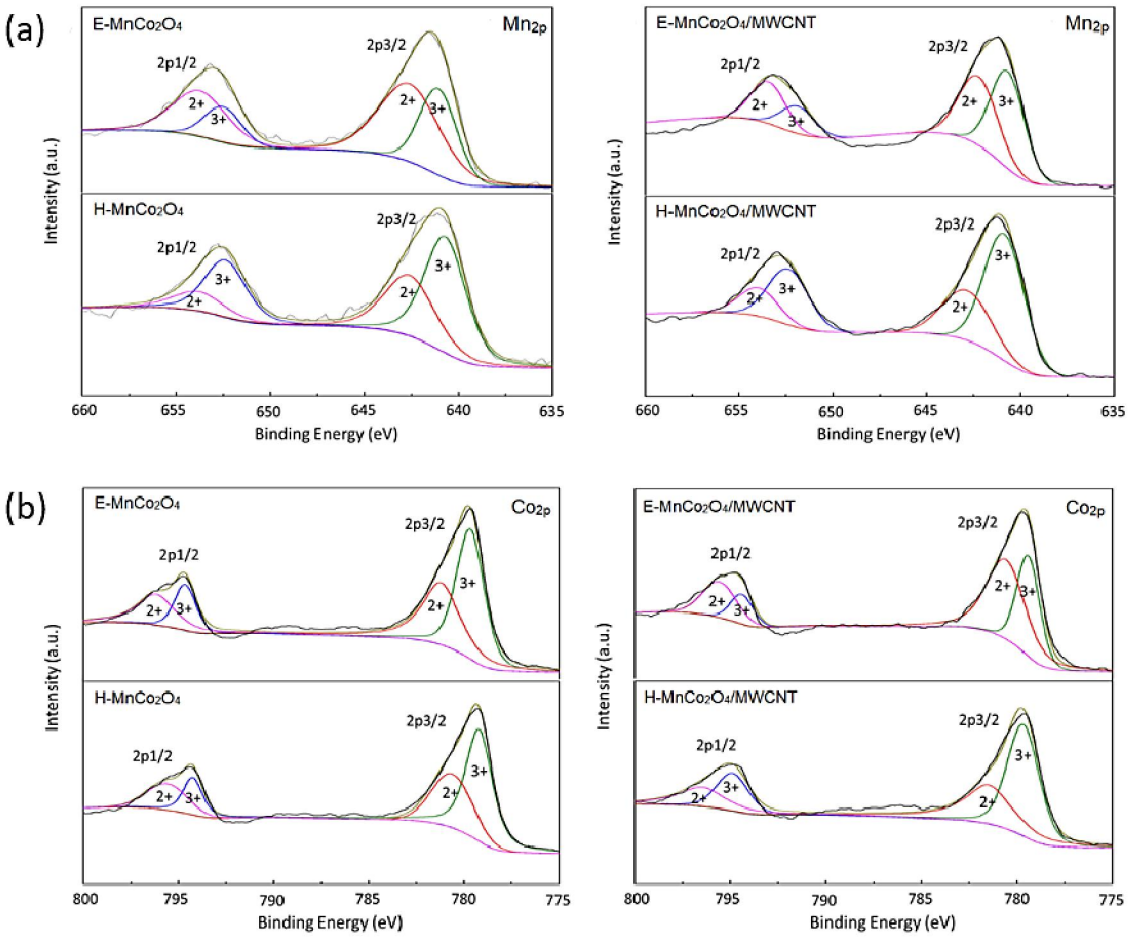

Figure 3 (a) the Mn2p core level spectra and (b) the Co2p core level spectra of E-$MnCo_2O_4$, H-$MnCo_2O_4$, E-$MnCo_2O_4$/MWCNT and H-$MnCo_2O_4$/MWCNT

X-ray photoelectron spectroscopy (XPS) analysis was operated to investigate the chemical composition of surfaces. As Figure 3 (a), the core level spectra of Mn_{2p} showed the prominent peaks at 652.18, 640.83 eV and 652.98, 640.88 eV of E-$MnCo_2O_4$ and H-$MnCo_2O_4$, respectively. Similar to E-$MnCo_2O_4$/MWCNT and H-$MnCo_2O_4$/MWCNT displayed the significant peaks at 652.98, 641.38 eV and 652.98, 641.18 eV, respectively. Those two main peaks correspond to the spin-orbit-split of Mn $2p_{1/2}$ and Mn $2p_{3/2}$. While the core level spectrum of cobalt (Co *2p*), shown in Figure 3 (b), exhibits the main peaks represented Co $2p_{1/2}$ (≈795) and Co $2p_{3/2}$ (≈780). These results show the presence of mixed both Mn^{2+}, Mn^{3+} and Co^{2+}, Co^{3+} [16]. Table 4.

The core-level spectrum of oxygen was presented in Figure 4. These deconvoluted results correspond to the surface oxygen and metal-oxygen bond in the metal oxide. Besides, the peaks in Figure 4 can be divided into three peaks. The red peak represented lattice oxygen or highly oxidative oxygen species (O^{2-} or O_2^{2-}/O^-). The green peak showed hydroxyl groups or the surface absorbed oxygen (-OH or O_2), and a blue peak is associated with absorbed molecular water [17].

Base on Table 1, we can clearly recognize that the lattice oxygen or highly oxidative oxygen species of $MnCo_2O_4$/MWCNT electrocatalysts show significantly larger the area under the graph than the pure $MnCo_2O_4$. The O^{2-} or O_2^{2-}/O^- of E-$MnCo_2O_4$ with MWCNT show 6.31% over E-$MnCo_2O_4$, while H-$MnCo_2O_4$/MWCNT present the higher O^{2-} or O_2^{2-}/O^- of H-$MnCo_2O_4$ (17.81%). Comparing with the fabrication methods, E-$MnCo_2O_4$/MWCNT shows the larger lattice oxygen / high-valent oxygen ion pair than H-$MnCo_2O_4$/MWCNT 3.23%. The lattice oxygen / high-valent oxygen ion pair (O^{2-} or O_2^{2-} / O^-) plays an important role in the oxygen precipitation reaction of the water decomposition process [17].

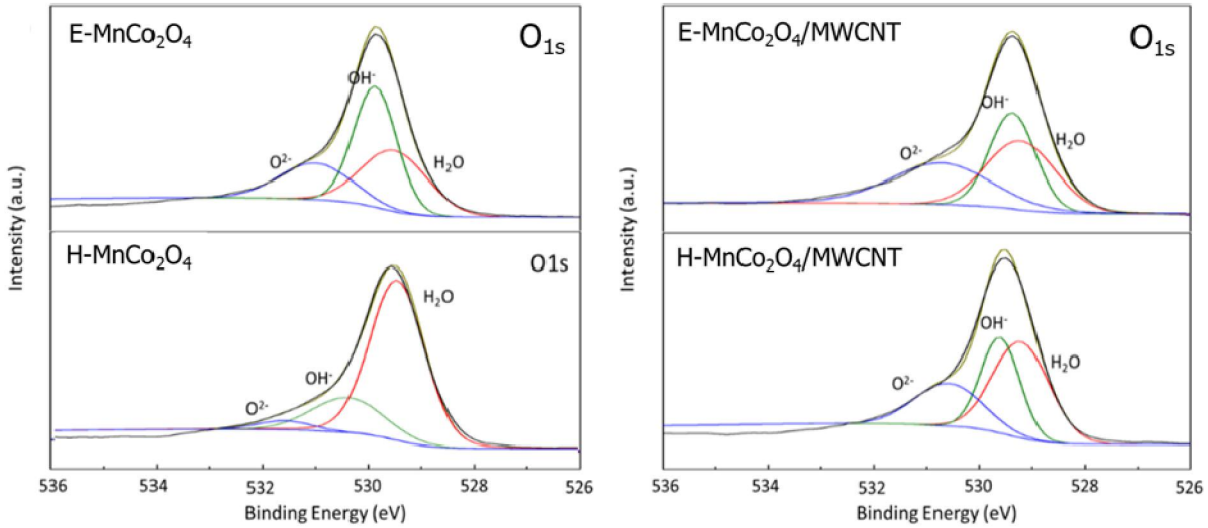

Figure 4 The oxygen core level spectra of E-$MnCo_2O_4$ and E-$MnCo_2O_4$/MWCNT, (b) H-$MnCo_2O_4$ and H-$MnCo_2O_4$/MWCNT

Table 1 O1s XPS peak deconvolution results

Electro-catalysts	O^{2-} or O_2^{2-}/O^-	-OH or O_2	H2O
H-$MnCo_2O_4$	12.37%	22.32%	65.31%
E-$MnCo_2O_4$	27.1%	42.6%	30.3%
H-$MnCo_2O_4$/MWCNT	30.18%	29.26%	40.56%
E-$MnCo_2O_4$/MWCNT	33.41%	31.64%	34.95%

To investigate the surface areas, Brunauer-Emmett-Teller (BET) technique was operated. As Figure 5 (a and b) show certain hysteresis loops of H-$MnCo_2O_4$/MWCNT and E-$MnCo_2O_4$/MWCNT in the adsorption and desorption curve of nitrogen, which indicates that pore structure appearing on the sample. Following Figure 5 (c), the specific surface area of H-$MnCo_2O_4$/MWCNT and E-$MnCo_2O_4$/MWCNT can be compared through the BET curve chart of obtained isotherm data from partial pressure range of 0.05 to 0.3. The specific surface area of E-$MnCo_2O_4$/MWCNT composite prepared by the electrospinning method is 67.85 m^2/ g, which is significantly larger than H-$MnCo_2O_4$/MWCNT composite prepared by hydrothermal method. (51.93 m^2/ g). The specific surface area of the catalyst plays a critical role in OER. A larger specific surface area indicates that the catalyst offers a more active site in the catalytic process. According to the BET test results, theoretically, E-$MnCo_2O_4$/MWCNT presented a better catalytic effect in OER than H-$MnCo_2O_4$/MWCNT. However, those prepared $MnCo_2O_4$/MWCNT composited catalysts also need to investigate further electrochemical measurements.

3.1 Electrochemical properties

Onset potential is the most significant factor for evaluating the performance of the OER catalyst. To investigate the onset potential of as prepared composite catalysts, a linear sweep voltammogram (LSV). Figure 6 (b) shows a current density of 0.1 mA/cm^2, which is considered to represent an onset potential required for catalytic processing. E-$MnCo_2O_4$/MWCNT was observed the significant lower onset potential (1.507 V) than those other; H-$MnCo_2O_4$/MWCNT (1.523 V), E-$MnCo_2O_4$ (1.525 V), and H-$MnCo_2O_4$ (1.528 V). Meanwhile, a noble metal oxide catalyst, IrO_2 shows the lowest onset potential (1.488 V). The onset potential value is very difficult to observe the exact values and use as a general possibility to compare the properties of catalysts reported in the literature. Therefore, the value of the over potential at 10 mA/cm^3 (E_j=10), is a value which is considered more reliable and commonly used.

As shown in Figure 6 (a), E-$MnCo_2O_4$/MWCNT exhibits the lowest over potential at approximately 0.52 V, which is significantly lower than H-$MnCo_2O_4$/MWCNT (0.54 V), E-$MnCo_2O_4$ (0.54 V), and H-$MnCo_2O_4$ (0.57 V). A smaller over potential indicates better catalytic activity for OER.

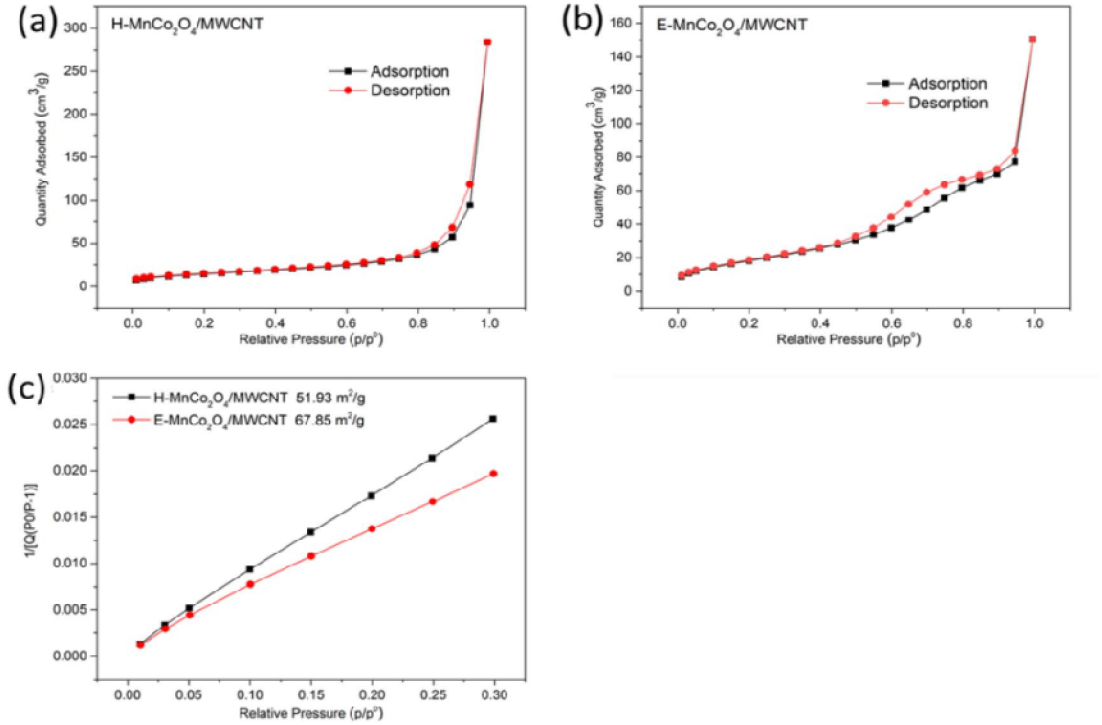

Figure 5. Nitrogen adsorption and desorption curves of catalyst (a) H-$MnCo_2O_4$/MWCNT, (b) E-$MnCo_2O_4$/MWCNT and (c) BET curves of three catalysts

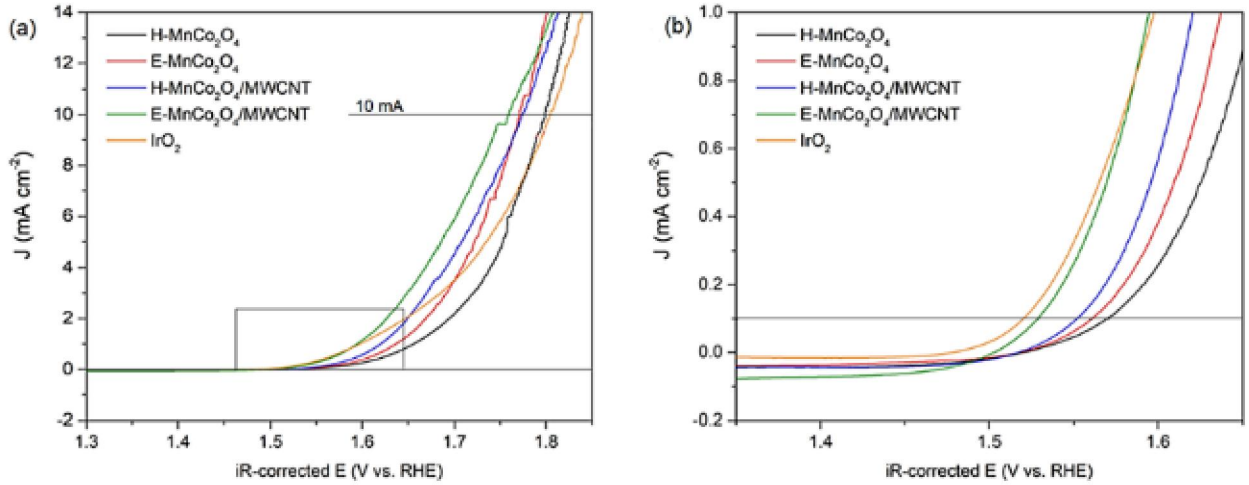

Figure 6. iR-corrected

The quality of good OER is that it should have a low Tafel slope and large current density. Following Figure 7, Tafel slopes of E-$MnCo_2O_4$/MWCNT (114.97 mV/dec) and E-$MnCo_2O_4$ (117.49 mV/dec) indicated lower than those samples prepared by the hydrothermal method, e.g., H-$MnCo_2O_4$/MWCNT (119.87 mV/dec) and H-$MnCo_2O_4$ (140.19 mV/dec).

EIS measurements are generally interpreted using a correlation between the impedance data and an equivalent circuit representing the physical processes

taking place in the system under investigation or through graphical representations. Figure 4.3 demonstrated the EIS curves of prepared catalysts.

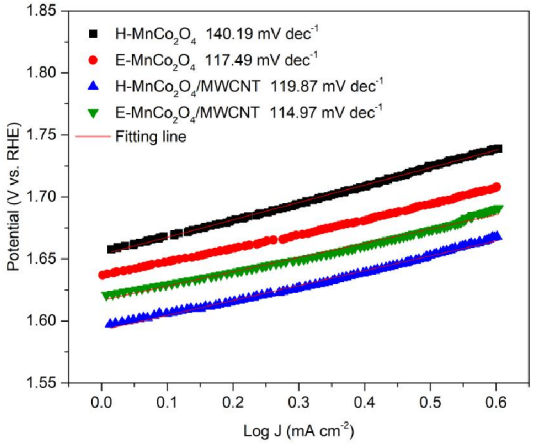

Figure 7. Tafel plots of H-MnCo2O4, H-MnCo2O4/ MWCNT, E-MnCo2O4, and E-MnCo2O4/MWCNT

The result showed a smaller semicircle of $MnCo_2O_4$/MWCNT composite than pure $MnCo_2O_4$ for both preparation methods; electrospinning and hydrothermal methods. E-$MnCo_2O_4$/MWCNT exhibited the lowest resistance, followed by H-$MnCo_2O_4$/MWCNT, which suggests that decorating MWCNT provides the potential to reduce the electrochemical impedance. Those also improve the electronic conductivity of the catalyst for OER [18].

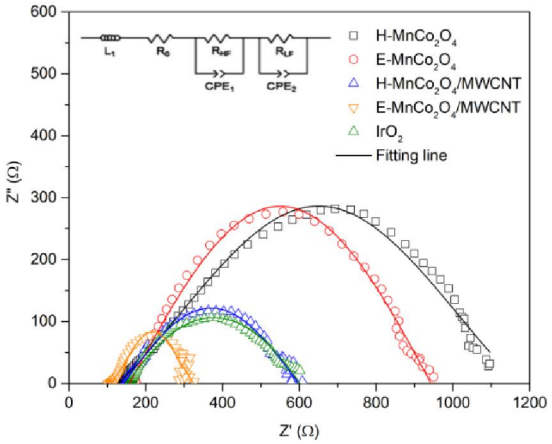

Figure 8. Electrochemical impedances of H-$MnCo_2O_4$, H-$MnCo_2O_4$/MWCNT, E-$MnCo_2O_4$, and E-$MnCo_2O_4$/ MWCNT catalysts

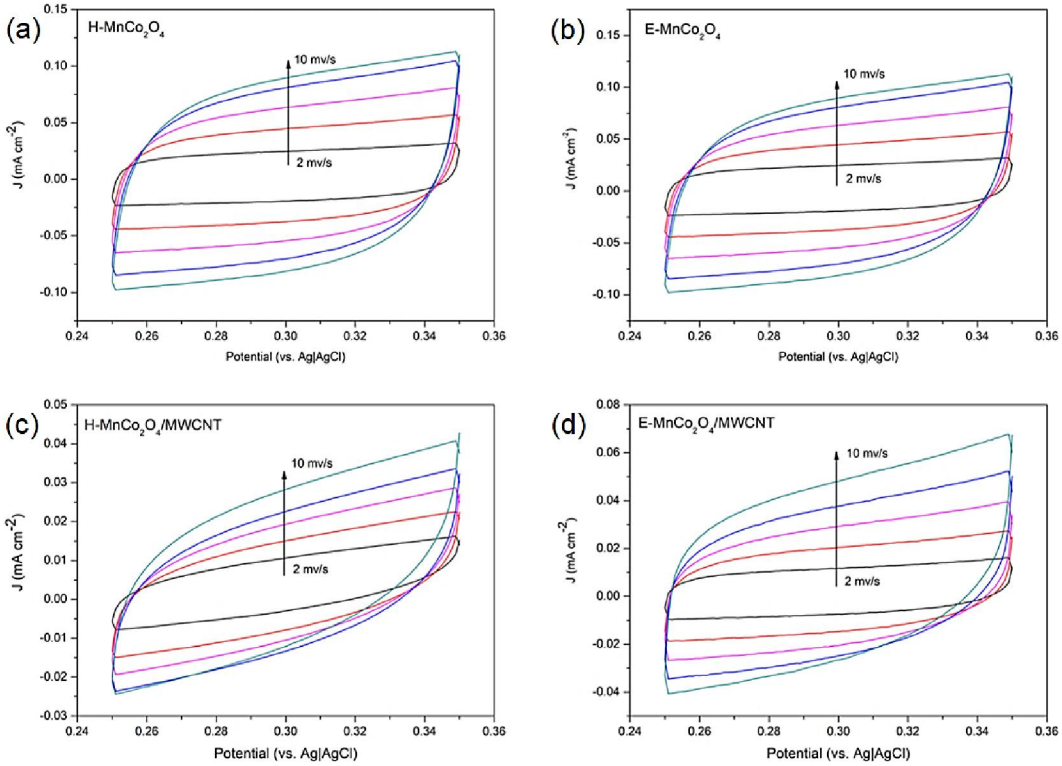

Figure 9. Cyclic voltammogram measurement of (a) H-$MnCo_2O_4$, (b) H-$MnCo_2O_4$/MWCNT, (c) E-$MnCo_2O_4$, and (d) E-$MnCo_2O_4$/MWCNT in different scan rates (2 to 10 mV/s)

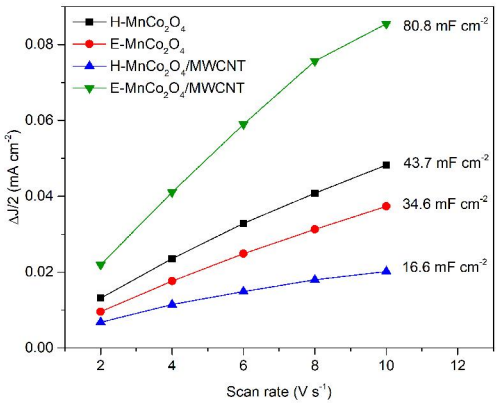

Figure 10. Electrochemical specific surface (ECSA) results in the function of scan rate.

The active surface area is the most important element of improving electro catalyst for OER. To investigate the perspective of electrochemical specific surface area for evaluating the exact active site of OER, Cyclic voltammograms (CV) measurements are often used to calculate the electrochemical surface area (ECSA) of electro catalysts [19]. In Figure 9, CV measurement is determined in the area of the current 0.35-0.45 V vs Ag (AgCl) with a scan rate of 2, 4, 6, 8 and 10 mV/s. Figure 10 presented the result based on the current density difference ($\Delta J/2 = (J_a-J_c)/2$) at 0.3 V vs. Ag | AgCl in the function of scan rate. The electrochemical double-layer capacitances (C_{dl}) result displayed the C_{dl} of H-$MnCo_2O_4$, H-$MnCo_2O_4$/MWCNT, E-$MnCo_2O_4$ and E-$MnCo_2O_4$/MWCNT is 43.7, 16.6, 34.6 and 80.8 mF/cm^2, respectively.

In practical applications, the stability of a catalyst is a major factor which is severely affected by various factors such as natural. The stability results of the samples are shown in Figure 11. The black curve in the figure represents an LSV before the accelerated cycle and the red curve denotes after the accelerated cycle. In terms of the decreased percentage of potential at 10 mA/s after accelerated 1000 cycles, the H-$MnCo_2O_4$ catalyst showed a decrease of 2.198 %. Meanwhile, H-$MnCo_2O_4$/MWCNT, E-$MnCo_2O_4$, and E-$MnCo_2O_4$/MWCNT composite catalyst displayed decreasing of 1.765 %, 5.814 % and 3.841 % respectively. In comparison, the H-$MnCo_2O_4$/MWCNT sample demonstrated stability greater than H-$MnCo_2O_4$ one. In the same directions, E-$MnCo_2O_4$/MWCNT also exhibited better stability than E-$MnCo_2O_4$. With these results can be suggested that decorating with MWCNT has an influence on the stability of an electro-catalyst. However, the stability of all samples in this study was presented with quite good stability after 1000 cycles.

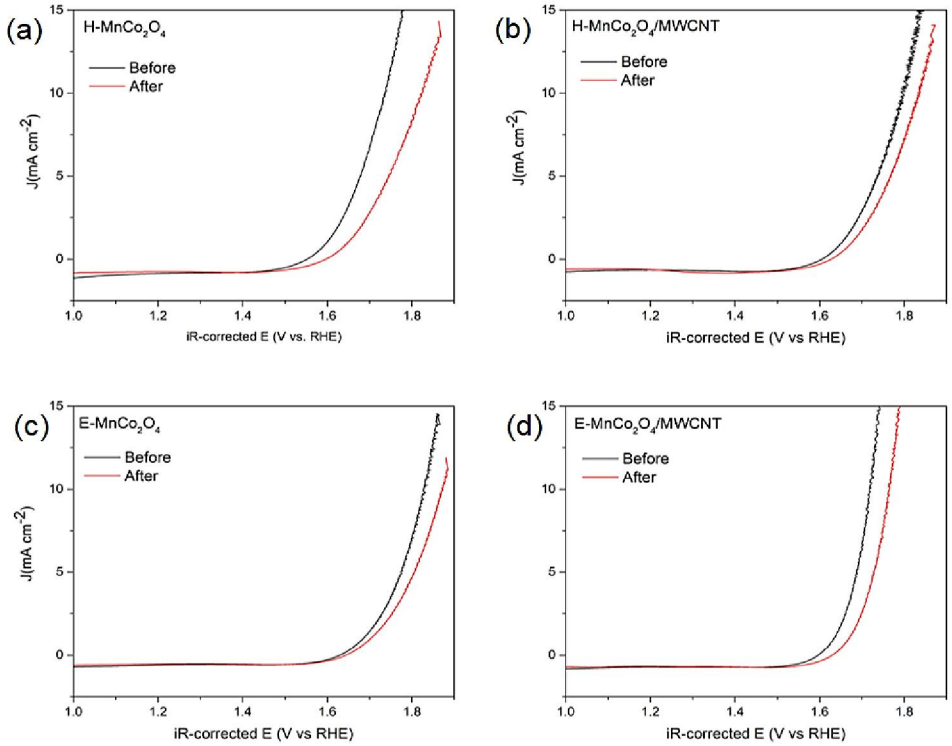

Figure 11. Electro-catalytic stability of (a) H-$MnCo_2O_4$, (b) H-$MnCo_2O_4$/MWCNT, (c) E-$MnCo_2O_4$ and (d) E-$MnCo_2O_4$/MWCNT composite catalysts after 1000 cycles

Following these, all results can be suggested that E-$MnCo_2O_4$/MWCNT provides better performance of OER. The morphology of catalyst prepared by the electrospinning method is in microfiber shape which offers a high specific area over other as-prepared catalysts. This is one of the essential factors for better OER. Additionally, the decoration of MWCNT directly affects the better OER. In terms of electrochemical properties, E-$MnCo_2O_4$/MWCNT shows the lowest onset potential, over potential, and Tafel slope comparing to others, while the ECSA value of E-$MnCo_2O_4$/MWCNT is much larger. To study and compare the electrochemical properties of as-prepared electro-catalyst will be contrasted with others to analyst the performance of electro-catalyst in several views.

4. Conclusion

In summary, the $MnCo_2O_4$ and $MnCo_2O_4$/MWCNT composite catalysts via both two preparation methods; hydrothermal and electrospinning were prepared. All experiment results can be suggested that E-$MnCo_2O_4$/MWCNT provides better performance of OER. The morphology of catalyst prepared by the electrospinning method is in microfiber shape which offers a high specific area over other as-prepared catalysts. This is one of the essential factors for better OER. Additionally, the decoration of MWCNT directly affects the better OER.

A designed electro-catalyst for enhancing OER required a catalyst that is able to overcome the large active energy at low potential. Although the catalytic materials are the most important issue, several parameters also significantly influence their reactions such as an electrode, electrolyte, onset/over potential, Tafel slope and stability. Additionally, the decoration of MWCNT directly affects the better OER. In terms of electrochemical properties, E-$MnCo_2O_4$/MWCNT shows the lowest onset potential, over potential, and Tafel slope comparing to others, while the ECSA value of E-$MnCo_2O_4$/MWCNT is much larger.

References

1. Lion Hirth. The market value of variable renewables: The effect of solar wind power variability on their relative price [J]. Energy Economics, 2013, 38: 218-236.
2. Jian-Kun He. Objectives and strategies for energy revolution in the context of tackling climate change [J]. Advances in Climate Change Research, 2015, 6(2): 101-107.
3. Aiping Yu, Victor Chabot, Jiujun Zhang. Electrochemical Supercapacitors for Energy Storage and Delivery: Fundamentals and Applications [B]. Boca Raton, 2013: 24-67.
4. Caineng Zou, Qun Zhao, Guosheng Zhang, et al. Energy revolution: From a fossil energy era to a new energy era [J]. Natural Gas Industry B, 2016, 3(1): 1-11.
5. Peng Gu, Mingbo Zheng, Qunxing Zhao, et al. Rechargeable zinc-air batteries: A promising way to green energy [J]. Journal of Materials Chemistry A, 2017, 5(17): 315487181.
6. Stefania Barca. Energy, property, and the industrial revolution narrative [J]. Ecological Economics, 2011, 715: 1309-1315.
7. Youngmin Lee, Jin Suntivich, Kevin Joseph May, et al. Synthesis and Activities of Rutile IrO_2 and RuO_2 Nanoparticles for Oxygen Evolution in Acid and Alkaline Solutions. Journal of Physical Chemistry Letters, 2012, 3(3): 399-404.
8. Fan Liao, Xingrong Han, Yanfei Zhang, et al., Hydrothermal synthesis of mesoporous $MnCo_2O_4$/$CoCo_2O_4$ ellipsoid-like microstructures for high-performance electrochemical super capacitor, Ceramics International 45 (2019) 7244-7252.
9. Ning Cai, Jing Fu, Vincent Chan, et al., $MnCo_2O_4$@nitrogen-doped carbon nanofiber composites with meso-microporous structure for high-performance symmetric supercapacitors [J]. Journal of alloys and compounds, 2019 (782): 251-262.
10. C. Chen, B. Liu, Q. Ru, S. Ma, B. An, X. Hou, S. Hu, Fabrication of cubic spinel MnCo2O4 nanoparticles embedded in graphene sheets with their improved lithium-ion and sodium-ion storage properties, J. Power Sources 326 (2016) 252–263.
11. L. Yao, J. Wu, H. Deng, Q.-A. Huang, Q. Su, G. Du, $MnCo_2O_4$/graphene composites anchored on Ni foam as binder-free anode with enhanced lithium-storage performance, Mater. Lett. 180 (2016) 188–191.
12. B. Saravanakumar, G. Ravi, V. Ganesh, et al, $MnCo_2O_4$ nanospheres synthesis for electrochemical applications, Material Science for Energy Technologies 2 (2019) 130-138.
13. Pranav Kulkarni, Debasis Ghosh, Geetha Balakrishna, et al. Investigation of $MnCo_2O_4$/MWCNT composite as anode material for lithium ion battery [J]. Ceramics International. 2019, 45(8): 10619-10625.
14. Md Abdul Wahab, Jickson Joseph, Luqman Atanda, et al. Nanoconfined synthesis of nitrogen-rich metal-free mesoporous carbon nitride electrocatalyst for the oxygen evolution reaction [J]. ACS Applied Energy Materials,

2020, (3)2: 1439-1447.
15. Yanjun Zhai, Hongzhi Mao, Peng Liu, et al. Facile fabrication of hierarchical porous rose-like $NiCo2O_4/MnCo_2O_4$ with enhanced electrochemical performance for energy storage [J]. Journal of Materials Chemistry A, 2015, (3): 16142–16149.
16. Jianwei Li, Dongbin Xiong, Linzhe Wang, et al. High-performance self-assembly $MnCo_2O_4$ nanosheets for asymmetric supercapacitors [J]. Journal of Energy Chemistry, 2019, 37: 66-72.
17. Hao Liu, Xifeng Ding, Lixi Wang, et al. Cation deficiency design: a simple and efficient strategy for promoting oxygen evolution reaction activity of perovskite electrocatalyst [J]. Electrochimica Acta, 2018, 259: 1004-1010.
18. Pravin Babar, Abhishek Lokhande, Myengil Gang, et al. Thermally oxidized porous NiO as an efficient oxygen evolution reaction (OER) electrocatalyst for electrochemical water splitting application [J]. Journal of Industrial and Engineering Chemistry, 2018, 60: 493-497.
19. Aso Navaee, Abdollah Salimi. Specific anion effects on copper surface through electrochemical treatment: Enhanced photoelectrochemical CO_2 reduction activity of derived nanostructures induced by chaotropic anions [J]. Applied Surface Science, 2018, 440(15): 897-906.
20. Mohamed Abdel Salam, Robert Burk. Synthesis and characterization of multi-walled carbon nanotubes modified with octadecylamine and polyethylene glycol [J]. Arabian Journal of Chemistry, 2017, S921-S927.

6/8/2020